Eur. Phys. J. B (2015) 88: 99
DOI: 10.1140/epjb/e2015-50849-3

THE EUROPEAN PHYSICAL JOURNAL B

Regular Article

Quartets and the current-phase structure of a double quantum dot superconducting bijunction at equilibrium

Denis Feinberg[1,2,a], Thibaut Jonckheere[3], Jérôme Rech[3], Thierry Martin[3], Benoît Douçot[4], and Régis Mélin[1,2]

[1] Centre National de la Recherche Scientifique, Institut NEEL, 38042 Grenoble Cedex 9, France
[2] Université Grenoble-Alpes, Institut NEEL, 38042 Grenoble Cedex 9, France
[3] Aix-Marseille Université, Université de Toulon, CNRS, CPT, UMR 7332, 13288 Marseille, France
[4] Laboratoire de Physique Théorique et des Hautes Energies, CNRS UMR 7589, Universités Paris 6 et 7, 4 place Jussieu, 75252 Paris Cedex 05, France

Received 10 December 2014 / Received in final form 3 March 2015
Published online 13 April 2015 –

Abstract. The equilibrium current-phase structure of a tri-terminal superconducting Josephson junction (bijunction) is analyzed as a function of the two relevant phases. The bijunction is made of two noninteracting quantum dots, each one carrying a single level. Nonlocal processes coupling the three terminals are described in terms of quartet tunneling and pair cotunneling. These couplings are due to nonlocal Andreev and cotunneling processes through the central superconductor S_0, as well as direct interdot coupling. In some cases, two degenerate midgap Andreev states appear, symmetric with respect to the (π, π) point. The lifting of this degeneracy by interdot couplings induces a strong non-local inductance at low enough temperatures. This effect is compared to the mutual inductance of a two-loop circuit.

1 Introduction

Josephson junctions couple two superconductors by an insulator or normal metal bridge N [1]. In the latter case, the Josephson effect in a two-terminal SNS junction relies on the coherence of the Andreev reflections at each NS interface, which results at equilibrium in the Andreev bound states (ABS). Two Andreev reflections, one at each interface, allow one Cooper pair to cross the SNS junction. The ABS dispersion with the phase difference at the junction essentially controls the current-phase (CPR) relationship of the junction. The CPR can be experimentally probed by SQUID interferometry [2], and, more recently, the ABS structure has been directly investigated by microwave spectroscopy [3,4]. Dot and double-dot set-ups can also be investigated by resonant coupling to a microwave cavity [5].

The present work focuses on the ABS structure at equilibrium of a tri-terminal Josephson [6–14]. It elucidates its current-phase relation as a function of the two phase variables, hence the name "bijunction". It clarifies the nature of several nonlocal processes occurring in such a structure. This current-phase relation could be probed by methods inspired by those used in the framework of two-terminal junctions. For instance, a two-loop biSQUID geometry has been recently proposed by us [15]. On the other hand, for transparent enough contacts, the Andreev bound states formed within the bijunction could be probed by spectroscopy tools [3,4], or, as recently suggested, using a closeby NS junction [16].

More specifically, we consider here the case of a bijunction (Fig. 1) where each arm is formed by a single level quantum dot [13], made for instance from a single carbon nanotube or nanowire. This structure is closely related to hybrid bijunctions made of two quantum dots and normal (instead of superconducting) reservoirs $N_{a,b}$, which have been fabricated either with carbon nanotubes or with semiconducting nanowires, in a $(N_a D_a S_0 D_b N_b)$ structure [17–21]. Indeed, nonlocal processes in double $(N_a S_0 N_b)$ hybrid structures connecting one superconductor S_0 to two normal metals $N_{a,b}$ have been predicted [22–30] and explored in experiments [18–21,31–33], with the prospect of producing entangled pairs of electrons. In the language of quasiparticle scattering, either an electron (hole) impinging on S_0 from N_a is normally transmitted as an electron (hole) towards S_b, or it is Andreev-transmitted as a hole (electron). The first channel corresponds to tunneling of a quasiparticle through the superconducting gap (so-called "elastic cotunneling" EC), while the second one involves the creation (annihilation) of a Cooper pair in S_0 and is a nonlocal (crossed) Andreev process (CAR). The latter amounts to split Cooper pairs into entangled singlets [26–29,34], and is responsible for nonlocal and spin-dependent conductance, while the proof of spin entanglement remains elusive. The experimental results clearly show the existence of nonlocal processes leading to splitting Cooper pairs from S_0 into pairs of quasiparticles in N_a, N_b.

[a] e-mail: denis.feinberg@neel.cnrs.fr

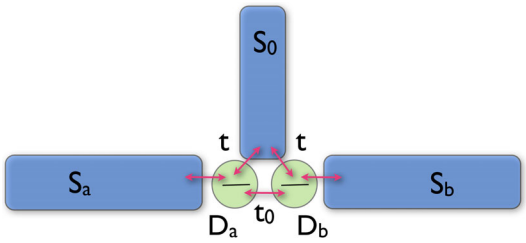

Fig. 1. Bijunction considered in this paper, made of two quantum dots D_a, D_b. The interdot ($t_{dd} = t_0$) and superconductor-dot ($t_{sd} = t$) hopping parameters are indicated.

In an all-superconducting bijunction, CAR and EC result in new coherent multipair transport channels, that must occur between the three terminals [6–9,13]. At equilibrium, in a bijunction, the combination of crossed Andreev process at S_0 and local Andreev reflection at $S_{a,b}$ builds ABS, which depend on *two* phase variables, say $\varphi_a - \varphi_0$, $\varphi_b - \varphi_0$. Those states can in particular mediate the simultaneous passage of *two* Cooper pairs from S_0 towards S_a, S_b, achieving so-called quartet transport.

In the present case of an all-superconducting tri-terminal set-up, these new processes introduce a microscopic coupling between the two junctions [9]. At equilibrium, the general picture is that of Andreev bound states coherently formed on both junctions a, b simultaneously. As a result, the total energy of the bijunction is a 2π-periodic function $E_{BJ} = E(\varphi_{0a}, \varphi_{0b})$ of the phase differences $\varphi_{0a} = \varphi_a - \varphi_0$ and $\varphi_{0b} = \varphi_b - \varphi_0$, and the currents

$$I_a = \frac{2e}{\hbar}\frac{\partial E_{BJ}}{\partial \varphi_{0a}}\,, \quad I_b = \frac{2e}{\hbar}\frac{\partial E_{BJ}}{\partial \varphi_{0b}} \tag{1}$$

are both functions of φ_{0a} *and* of φ_{0b}. In this work we derive the exact current-phase relationship (CPR) in a two-dot bijunction. Due to the tri-terminal geometry, nontrivial midgap states may appear, symmetric with respect to the central (π, π) point. The importance of such states has been recently underlined in reference [35]. We show how the underlying degeneracy is lifted by interdot couplings, directly or through the central superconductor. This understanding of the CPR should clarify the nature of the nonequilibrium transport, which offers new coherent dc channels in presence of applied voltages, provided the latter are commensurate [6,9,13], and also nonlocal multiple Andreev incoherent channels [7,8]. Subgap anomalies in a diffusive Al-Cu bijunction have indeed been recently observed and interpreted in terms of quartets (see Fig. 8b) [14]. Notice that a related set-up has been proposed in the context of Majorana fermion physics [36].

Section 2 defines the model and the exact solution for the ABS, that becomes analytic in the low energy limit. Section 3 discusses the structure of the ABS states of the bijunction, first in the analytic limit. Section 4 provides a discussion of the currents and the resulting nonlocal inductance in the general case, and also considers the role of the circuit inductances when the phases are imposed by a two-loop set-up.

2 Bijunction with two quantum dots: the model

Each junction $S_{a(b)} - S_0$ is formed by a quantum dot $D_{a(b)}$ with a single noninteracting level, with energies $E_{a(b)}$ respectively, and a direct coupling between the single levels in $D_{a(b)}$ in the electron-electron channel (Fig. 1). Such a coupling is a simplified way to modelize the connectivity of the nanotube [20,34]. The Hamiltonian of the system is written in the Nambu notation $H = H_S + H_{DD} + H_T$, and performing a gauge transformation to incorporate the superconducting phases φ_j in the tunneling term H_T:

$$H_S = \sum_{j=a,b,0}\sum_k \Psi_{jk}^\dagger(\xi_k\sigma_z + \Delta_j\sigma_x)\Psi_{jk}, \Psi_{jk} = \begin{pmatrix} \psi_{jk,\uparrow} \\ \psi_{j(-k),\downarrow}^\dagger \end{pmatrix} \tag{2}$$

$$H_{DD} = \sum_{\alpha=a,b} E_\alpha d_\alpha^\dagger \sigma_z d_\alpha + t_{dd}\,[d_b^\dagger \sigma_z d_a + h.c.] \tag{3}$$

$$H_T = \sum_{jk\alpha} \Psi_{jk}^\dagger T_{j\alpha} d_\alpha + h.c., \qquad d_\alpha = \begin{pmatrix} d_{\alpha\uparrow} \\ d_{\alpha\downarrow}^\dagger \end{pmatrix}, \tag{4}$$

with $T_{j\alpha} = t_{j\alpha}\sigma_z e^{i\sigma_z\varphi_j/2}$ and $t_{j\alpha}$ is the tunnelling amplitude between the lead j and dot α.

The vector connecting the (point) junctions $a - S_0$ and $S_0 - b$ is denoted as $\mathbf{R}$, and k_F is the Fermi vector in S_0. The procedure to obtain the Andreev bound states and the current-phase relationships by writing an effective action for the two dots is found in reference [37]. One expresses the partition function as

$$Z = \int \mathcal{D}\left[\bar\psi, \psi, \bar d, d\right] e^{-S\left[\bar\psi,\psi,\bar d,d\right]}, \tag{5}$$

e.g. as a functional integral over Grassmann fields for the electronic degrees of freedom $(\Psi, \bar\Psi, d, \bar d)$. The Euclidean action reads:

$$S_A = S_D + \int_0^\beta d\tau \times \left[\sum_{jk} \bar\Psi_{jk}(\tau)(\partial_\tau + \xi_k\sigma_z + \Delta_j\sigma_x)\Psi_{jk}(\tau) + H_T(\tau)\right]. \tag{6}$$

β is the inverse temperature, and $H_T(\tau) = \sum_{jk} \bar\Psi_{jk\alpha}(\tau) T_{j\alpha} d_\alpha(\tau) + h.c.$ while

$$S_D = \int_0^\beta d\tau \left[\sum_\alpha \bar d_\alpha(\partial_\tau + \epsilon_\alpha\sigma_z)d_\alpha + t_{dd}\,(d_b^\dagger\sigma_z d_a + h.c.)\right]. \tag{7}$$

After integrating out the leads we get $Z = \int \mathcal{D}[d_\alpha \bar d_\alpha] e^{-S_{eff}}$ with

$$S_{eff} = S_D - \int_0^\beta d\tau d\tau' \sum_{\alpha\delta} \bar d_\alpha(\tau)\check\Sigma_{\alpha\delta}(\tau - \tau')d_\delta(\tau') \tag{8}$$

where

$$\check{\Sigma}_{\alpha\delta}(\tau) = \sum_{j=a,b,0} T^{\dagger}_{j\alpha} G_{j,\alpha\delta}(\tau) T_{j\delta} \tag{9}$$

$$G_{j,\alpha\alpha}(\tau) = \sum_{k} (\partial_\tau + \xi_k \sigma_z + \Delta_j \sigma_x)^{-1} \delta(\tau) \tag{10}$$

$$G_{0,ab}(\tau) = \sum_{k} e^{i\mathbf{kR}} (\partial_\tau + \xi_k \sigma_z + \Delta_0 \sigma_x)^{-1} \delta(\tau). \tag{11}$$

We perform a Fourier transform on the Matsubara frequencies (with $\omega_n = (2n+1)\pi/\beta$): $\delta(\tau) = \frac{1}{\beta}\sum_{\omega_n} e^{-i\omega_n \tau}$ and $G(\tau) = \frac{1}{\beta}\sum_{\omega_n} e^{-i\omega_n \tau} G(i\omega_n)$, which gives for the Green's function G_j in terminal S_j:

$$\begin{aligned} G_j(i\omega_n) &= \int d\xi\ \nu(\xi)(-i\omega_n + \xi_k \sigma_z + \Delta_j \sigma_x)^{-1} \\ &\simeq \frac{\pi\nu(0)}{\sqrt{\Delta_j^2 - (i\omega_n)^2}} (i\omega_n + \Delta_j \sigma_x) \end{aligned} \tag{12}$$

and the nonlocal Green's functions connecting the junctions a, b on the distance R in a one-dimensional channel within terminal S_0,

$$\begin{aligned} G_{ab}(\omega_n) \simeq\ & e^{-R/\xi(i\omega_n)} \pi\nu(0) \\ & \times \left[\frac{i\omega_n + \Delta_0 \sigma_x}{\sqrt{\Delta_0^2 - (i\omega_n)^2}} \cos(k_F R) + \sigma_z \sin(k_F R) \right]. \end{aligned} \tag{13}$$

Here $\xi(i\omega_n) = \frac{\xi_0}{\sqrt{\Delta_0^2 - (i\omega_n)^2}}$ and $\nu(\xi) = \sum_k \delta(\xi - \xi_k)$ is approximated by a constant $\nu(0)$, the density of states at the Fermi level in the normal leads. Let us set the phase φ_0 to zero, and assume for sake of simplicity all gaps to be equal, $\Delta_j = \Delta$, and the two junctions equivalent, $t_{aa} = t_{0a} = t_{0b} = t_{bb} = t_{sd}$. This yields the self-energy as a matrix in the Nambu-dots four-dimensional space:

$$\check{\Sigma}_{\alpha\alpha}(i\omega_n) = \frac{\Gamma}{2\sqrt{\Delta^2 - (i\omega_n)^2}} \left[i\omega_n - \frac{\Delta}{2}(1 + e^{i\varphi_\alpha}) \sigma_x \right] \tag{14}$$

$$\begin{aligned} \check{\Sigma}_{ab}(i\omega_n) =\ & e^{-R/\xi(i\omega_n)} \\ & \times \frac{\Gamma}{4} \left[\frac{i\omega_n + \Delta\sigma_x}{\sqrt{\Delta^2 - (i\omega_n)^2}} \cos(k_F R) + \sigma_z \sin(k_F R) \right] \end{aligned} \tag{15}$$

with $\Gamma = 2\pi\nu(0) t_{sd}^2$. Introducing $d_\alpha(\tau) = \frac{1}{\sqrt{\beta}} \sum_{\omega_n} e^{-i\omega_n \tau}$ $d_\alpha(i\omega_n)$ and $\bar{\mathbf{d}} = (\bar{d}_a, \bar{d}_b)$, we finally obtain the effective action

$$\begin{aligned} S_{\mathit{eff}} &= \sum_{\omega_n} \bar{\mathbf{d}}(i\omega_n) \check{\mathbf{M}}(i\omega_n) \mathbf{d}(i\omega_n) \\ \check{\mathbf{M}}(i\omega_n) &= (-i\omega_n + \epsilon_\alpha \sigma_z) \check{\mathbf{I}}_{dot} - \check{\mathbf{\Sigma}}_{i\omega_n}, \end{aligned} \tag{16}$$

where $\check{\mathbf{M}}(i\omega_n)$ is described by a 4×4 matrix, whose coefficients are given by

$$\begin{aligned} M_{11} &= i\omega_n \left(1 + \frac{\Gamma}{2\sqrt{\Delta^2 - (i\omega_n)^2}} \right) - E_a, \\ M_{22} &= i\omega_n \left(1 + \frac{\Gamma}{2\sqrt{\Delta^2 - (i\omega_n)^2}} \right) + E_a, \\ M_{33} &= i\omega_n \left(1 + \frac{\Gamma}{2\sqrt{\Delta^2 - (i\omega_n)^2}} \right) - E_b, \\ M_{44} &= i\omega_n \left(1 + \frac{\Gamma}{2\sqrt{\Delta^2 - (i\omega_n)^2}} \right) + E_b, \\ M_{12} &= -\frac{\Gamma\Delta}{4\sqrt{\Delta^2 - (i\omega_n)^2}} (1 + e^{-i\varphi_a}), \\ M_{13} &= \frac{\Gamma}{4} e^{-R/\xi(i\omega_n)} \\ &\quad \times \left[\frac{i\omega_n}{\sqrt{\Delta^2 - (i\omega_n)^2}} \cos(k_F R) + \sin(k_F R) \right] + t_{dd}, \\ M_{14} &= M_{23} = -\frac{\Gamma}{4} e^{-R/\xi(i\omega_n)} \left[\frac{\Delta}{\sqrt{\Delta^2 - (i\omega_n)^2}} \cos(k_F R) \right], \\ M_{24} &= \frac{\Gamma}{4} e^{-R/\xi(i\omega_n)} \\ &\quad \times \left[\frac{i\omega_n}{\sqrt{\Delta^2 - (i\omega_n)^2}} \cos(k_F R) - \sin(k_F R) \right] - t_{dd}, \\ M_{34} &= -\frac{\Gamma\Delta}{4\sqrt{\Delta^2 - (i\omega_n)^2}} (1 + e^{-i\varphi_b}), \end{aligned} \tag{17}$$

$\check{\mathbf{M}}$ being an hermitian matrix once $i\omega_n$ is replaced by the real number z. Notice the normal and anomalous couplings between dots, featured by the matrix elements M_{ij} with $i = 1, 2$ and $j = 3, 4$. The dispersion relation for the ABS is given by the eigenvalues of the effective action, replacing $i\omega_n$ by z.

After integrating out the $\{d_\alpha, \bar{d}_\alpha\}$ variables, the partition function is given by

$$Z = \int \mathcal{D}\left[d_\alpha \bar{d}_\alpha\right] \ \ e^{-S_{\mathit{eff}}(d_\alpha, \bar{d}_\alpha)} = \prod_{i\omega_n} \det \check{\mathbf{M}}(\omega_n). \tag{18}$$

The free energy reads:

$$F = -\frac{1}{\beta} \sum_{\omega_n} \ln(\det \check{\mathbf{M}}(i\omega_n)). \tag{19}$$

The Josephson current in S_a is expressed as:

$$I_{Ja,b} = \frac{2e}{\hbar} \frac{\partial F}{\partial \varphi_{a,b}} = -\frac{2}{\beta} \frac{\partial}{\partial \varphi_{a,b}} \sum_{\omega_n} \ln(\det \check{\mathbf{M}}(i\omega_n)). \tag{20}$$

One can further define an *intrinsic* inductance matrix $\mathbf{L}$ such as the elements of the inverse inductance matrix $\mathbf{\Lambda} = \mathbf{L^{-1}}$ are given by:

$$\Lambda_{aa} = \frac{\partial I_{Ja}}{\partial \varphi_a}, \ \ \Lambda_{bb} = \frac{\partial I_{Jb}}{\partial \varphi_b}, \ \ \Lambda_{ab} = \frac{\partial I_{Ja}}{\partial \varphi_b}, \ \ \Lambda_{ba} = \frac{\partial I_{Jb}}{\partial \varphi_a}. \tag{21}$$

$$\check{\mathbf{M}}(i\omega_n) = \begin{pmatrix} i\omega_n - E_a & -\frac{\Gamma}{4}(1+e^{-i\varphi_a}) & t & \bar{t} \\ -\frac{\Gamma}{4}(1+e^{i\varphi_a}) & i\omega_n + E_a & \bar{t} & -t \\ t & \bar{t} & i\omega_n - E_b & -\frac{\Gamma}{4}(1+e^{-i\varphi_b}) \\ \bar{t} & -t & -\frac{\Gamma}{4}(1+e^{i\varphi_b}) & i\omega_n + E_b \end{pmatrix} \tag{23}$$

3 Analytical solution in the large gap limit

In most cases, the contribution to the Josephson current of the continuum states ($|\omega| > \Delta$) is small, therefore one can easily infer the current-phase characteristics from the phase derivatives of the ABS energies. This becomes exact in the so-called large gap limit. One can indeed obtain an analytical solution in the limit $|E_{a,b}|, \Gamma, t_{dd} \ll \Delta$. This amounts to drop in $\check{\mathbf{M}}$ (Eq. (17)) the frequencies $i\omega_n$ in the denominators $\sqrt{\Delta^2 - (i\omega_n)^2}$, the factor $i\omega_n$ in $\check{\mathbf{M}}_{13}, \check{\mathbf{M}}_{24}$ as well as the renormalization factor $1+\frac{\Gamma}{2\Delta}$ in the diagonal elements. Defining

$$t = \frac{\Gamma}{4} e^{-R/\xi} \sin(k_F R) + t_{dd}, \quad \bar{t} = -\frac{\Gamma}{4} e^{-R/\xi} \cos(k_F R), \tag{22}$$

one obtains:

see equation (23) above

and solving the secular equation $\mathrm{Det}(\check{\mathbf{M}}) = 0$ yields the phase dispersion of the ABS cooperatively formed on the two dots, $\mathcal{E}_n = \pm\sqrt{z}$ $(n = 1, 2, 3, 4)$ with

$$\begin{aligned} z = {} & \frac{1}{2}(E_a^2 + E_b^2) + t^2 + \bar{t}^2 + \frac{\Gamma^2}{8}\left(\cos^2\frac{\varphi_a}{2} + \cos^2\frac{\varphi_b}{2}\right) \\ & \pm \Bigg\{ \left[E_a^2 - E_b^2 + \frac{\Gamma^2}{8}(\cos\varphi_a - \cos\varphi_b)\right]^2 \\ & + 2\Gamma^2\bar{t}^2\left(\cos^2\frac{\varphi_a}{2} + \cos^2\frac{\varphi_b}{2}\right) \\ & + \Gamma^2\left[t^2\sin^2\left(\frac{\varphi_a - \varphi_b}{2}\right) - \bar{t}^2\sin^2\left(\frac{\varphi_a + \varphi_b}{2}\right)\right] \\ & + 8t\bar{t}\Gamma\left(E_a\cos^2\frac{\varphi_b}{2} + E_b\cos^2\frac{\varphi_a}{2}\right) \\ & + 4t^2(E_a + E_b)^2 + 4\bar{t}^2(E_a - E_b)^2 \Bigg\}^{\frac{1}{2}}. \end{aligned} \tag{24}$$

The parameter t reflects the interdot couplings in the normal channel, both through S_0 and by direct tunneling (respectively first and second terms in Eq. (22)), and the parameter $\bar{t}$ represents the anomalous channel through S_0. The S_0 channels have a dependence in R, both oscillating at the Fermi wavevector and exponentially damped over the coherence length ξ. Notice that even in the case where $R \gg \xi$ such that nonlocal effects (CAR and EC) are negligible, the interdot coupling plays an essential role, making the bijunction different from two junctions in series. This situation may happen for instance with carbon nanotubes when the central superconducting finger is wide enough but weakly perturbs the nanotube. Let us now discuss the main features of the ABS spectrum within the large gap analytical solution, postponing the general discussion to the next section.

3.1 The nonresonant regime

In the case of uncoupled junctions (S_0S_a), (S_0S_b), e.g. for $t = \bar{t} = 0$, the ABS dispersion for each of the junctions is:

$$\mathcal{E}_{a(b),\pm} = \pm\sqrt{E_{a(b)}^2 + \frac{\Gamma^2}{4}\cos^2\frac{\varphi_{a(b)}}{2}}. \tag{25}$$

In the nonresonant regime $\Gamma \ll |E_{a(b)}|$ it yields a sinusoïdal current-phase relationship

$$\mathcal{E}_{a,b,\pm} \simeq \pm\left[E_{a(b)} + \frac{\Gamma^2}{16|E_{a(b)}|}(1 + \cos\varphi_{a,b})\right]. \tag{26}$$

If $E_b = \pm E_a$, the ABS in junctions a, b are degenerate. Switching on the nonlocal couplings EC and CAR as well as a possible direct interdot coupling t_{dd} hybridizes the two ABS doublets, yielding a set of four ABS $(n = 1{-}4)$ with $\mathcal{E}_{1,2} < 0$ and $\mathcal{E}_3 = -\mathcal{E}_1, \mathcal{E}_4 = -\mathcal{E}_2$, coherently delocalized over the two dots. It is illustrative to perform a perturbative expansion in Γ and the interdot couplings t, $\bar{t}$ of expression (24), which reduces at $T = 0$ to the following approximate expression for the total energy of the bijunction (up to an irrelevant constant):

$$\begin{aligned} E_{BJ} = {} & -E_0[\cos\varphi_a + \cos\varphi_b] - E_0'[\cos 2\varphi_a + \cos 2\varphi_b] \\ & - E_Q\cos(\varphi_a + \varphi_b) - E_{PC}\cos(\varphi_a - \varphi_b). \end{aligned} \tag{27}$$

The first term reflects the "local" tunnel terms of single junctions a, b $(E_0 > 0)$. The second term is the next harmonic, featuring two pairs passing through a, or through b $(E_0' < 0)$. The third and the fourth terms respectively describe quartet tunneling (from S_0 towards S_a, S_b) and pair cotunneling from S_a to S_b. The quartet term is a novel contribution that does not appear in Josephson networks. Expression (27) yields the inverse inductance Λ_{ab}

$$\Lambda_{ab} = \frac{2e}{\hbar}[E_Q\cos(\varphi_a + \varphi_b) - E_{PC}\cos(\varphi_a - \varphi_b)]. \tag{28}$$

On the lines $\varphi_a = \pm\varphi_b = \varphi$ in the (φ_a, φ_b) plane, Λ_{ab} oscillates with period π with one of the phases (say φ_b). One obtains

$$E_Q \approx -\frac{\Gamma^2\bar{t}^2}{64E_0^4}, \quad E_{PC} \approx \frac{\Gamma^2 t^2}{64E_0^4} \tag{29}$$

(assuming $E_a = E_b = E_0$). One sees that E_{PC} is positive, just as an effective Josephson junction connecting S_a

and S_b, but on the contrary E_Q is *negative*. This means that in terms of quartet tunneling, which depends on the phase combination $\varphi_a + \varphi_b$, the weakly transparent bijunction is a π junction, which here means that the lowest energy is obtained for $\varphi_a + \varphi_b = \pi$.

This minus sign was discovered in reference [13] for the biased bijunction, close to equilibrium, and it comes from the antisymmetry of the Cooper pair wavefunction. Indeed, the quartet mechanism consists in forming two entangled singlet pairs in the dots a, b by a double CAR process. The result of this process is the production of two identical split pairs. Fermion exchange and recombination of these two split pairs into one pair in S_a and one pair in S_b introduces a minus sign. These current components can be probed by applying small voltages $V_{a,b}$ to reservoirs S_a, S_b ($V_0 = 0$) [9,13]. Then the phases become time-dependent, $\varphi_a = \varphi_{0a} + \frac{2e}{\hbar}V_a t$ and $\varphi_b = \varphi_{0b} + \frac{2e}{\hbar}V_b t$. In the adiabatic approximation, those time-dependent phases are simply substituted into equation (27). With $V_a = -V_b = V$, one obtains the π-shifted d.c. quartet current $I_Q = -I_{Q0}\sin(\varphi_{a0} + \varphi_{b0})$, which is *time-independent*. If one instead fixes $V_a = V_b = V$, one obtains the coherent pair transfer term $I_{PC} = I_{PC0}\sin(\varphi_{a0} - \varphi_{b0})$, resembling a standard d.c. Josephson term.

Notice that in a strongly nonresonant regime, $t, \bar{t}, \Gamma \ll E_{a,b}$, the ABS dispersion becomes independent on the relative signs of E_a and E_b. This means that, contrarily to the hybrid splitter ($N_a D_a S_0 D_b N_b$), tuning the levels to $E_a = \pm E_b$ does not help filtering any or the other of EC and CAR processes. This is due to the Andreev reflection which mixes electrons at energy E and holes at energy $-E$.

3.2 The resonant regime

Let us now turn to the resonant case, $E_a = E_b = 0$. Then the ABS dispersion in each junction $a(b)$ alone crosses zero energy at $\varphi_{a(b)} = \pi$. The resulting four-fold degeneracy is lifted by the interdot coupling, in a nonperturbative way. Let us focus on the diagonal directions in the phase plane. First, if $\varphi_a = \varphi_b = \varphi$, one finds (one defines $\tilde{t} = \sqrt{t^2 + \bar{t}^2}$)

$$E = \pm\sqrt{\tilde{t}^2 + \left(\frac{\Gamma^2}{4} \pm \Gamma\bar{t}\right)\cos^2\frac{\varphi}{2}} \qquad (30)$$

showing a structure similar to that of a single dot junction, where $\tilde{t}$ plays the role of an effective level energy and with an effective coupling $\Gamma\sqrt{1 \pm \frac{4\bar{t}}{\Gamma}}$ if $4\bar{t} < \Gamma$ which is satisfied from equation (17). In the case of no direct interdot coupling, $\tilde{t} = \frac{\Gamma}{4}e^{-R/\xi_0}$ does not depend on the geometrical phase $\beta_R = k_F R$, contrarily to the couplings t and $\bar{t}$ separately. Equation (30) can be interpreted in terms of "molecular states" formed on the double dot, due to the interdot couplings t and $\bar{t}$ (direct and through CAR and EC) with a degeneracy lifted by the local couplings to the superconductors, represented by Γ (Fig. 2, left panels). The scale of the splitting is given by $\tilde{t}$.

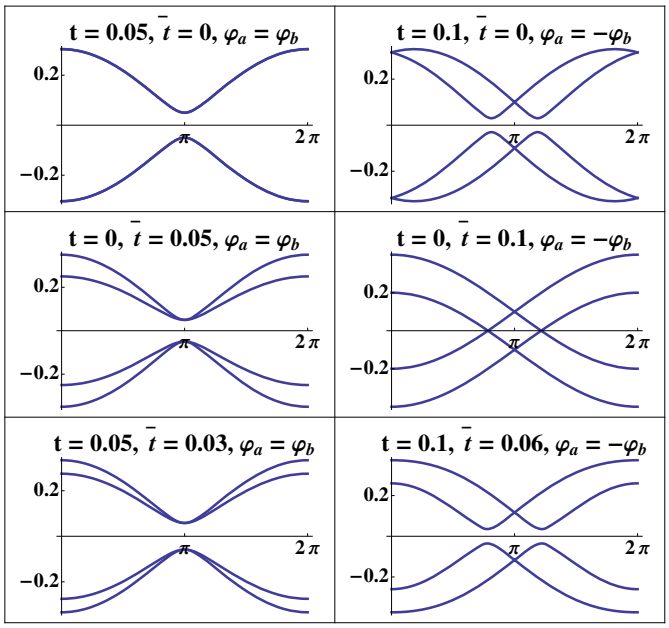

Fig. 2. Andreev bound state dispersion $E(\varphi)$ for the bijunction in the resonant case $E_a = E_b = 0$, in the large gap approximation, showing the lifting of the degeneracy by the interdot couplings, either at $\varphi = \pi$ along the line $\varphi_a = \varphi_b = \varphi$, or at $\varphi \neq \pi$ on the line $\varphi_a = -\varphi_b = \varphi$. $\Gamma = 0.6\Delta$.

On the other hand, in the case $\varphi_a = -\varphi_b = \varphi$, one obtains:

$$E = \pm\sqrt{\tilde{t}^2 + \frac{\Gamma^2}{4}\cos^2\frac{\varphi}{2} \pm \Gamma\left|\cos\frac{\varphi}{2}\right|\left(\bar{t}^2 + t^2\sin^2\frac{\varphi}{2}\right)^{1/2}}. \qquad (31)$$

In the peculiar case $t = 0$, which can be achieved if $t_{dd} = 0$ and $\beta_R = n\pi$, the dots are coupled only in the electron-hole channel, and the solution presents two twofold degenerate crossing points $E = 0$, at $\varphi = \pi \pm 2\arcsin\left(\frac{2\bar{t}}{\Gamma}\right)$. Coupling in the electron-electron channel by the parameter t lifts this degeneracy, leaving a two-gap structure (Fig. 2, right panels). This kind of degeneracy lifting is qualitatively different from that encountered along the other diagonal $\varphi_a = \varphi_b$, where the $E = 0$ crossing instead occurs at (π, π). Indeed the scale of the phase splitting of the crossing points is given by $\tilde{t}/\Gamma$. Yet the energy splitting at those crossing points is of the order of $2\frac{t}{\Gamma}\tilde{t}$, thus these minigaps are much smaller than the one formed at $\varphi = \pi$ in the case $\varphi_a = \varphi_b$. To complete this picture, a case close to resonance is represented in Figure 3.

Several remarks must be made in the resonant regime. First, it is no more possible to distinguish between quartet and pair cotunneling processes. Just as in a single transparent *SNS* junction couples two superconductors by a strongly nonperturbative proximity effect in the N region, the bijunction ensures a coupling between three superconductors by proximity effect in the double dot. Second, due to lifting of the four-fold degeneracy, the sharp qualitative change between the individual ABS and the full bijunction structure holds at $T = 0$ for any, whatever weak, interdot

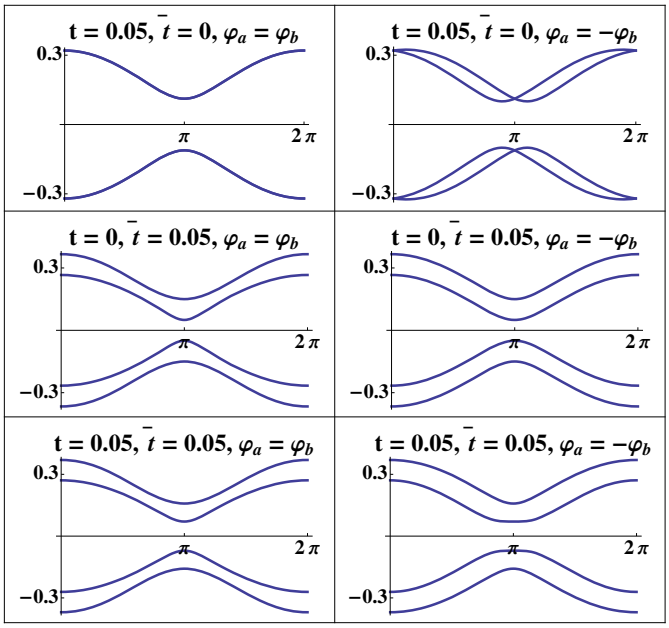

Fig. 3. Same parameters as in Figure 2 but in a slightly nonresonant case, $E_a = -E_b = 0.1\Delta$.

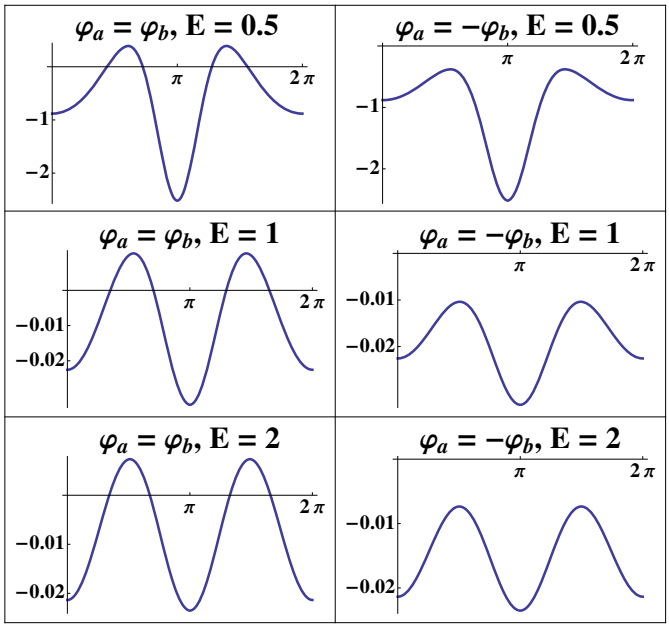

Fig. 4. Exact solution: nonlocal inverse inductance $\Lambda_{ab}(\varphi_b)$ ($\times 10^3$) in the nonresonant regime, for $\Gamma = \Delta$, $T = 0.05\Delta$, $R = \xi$, $\beta_R = \frac{\pi}{7}$ and $E_a = \pm E_b = E$.

coupling, including the case of a wide ($R \gg \xi$) central superconductor.

4 General discussion

4.1 Current-phase relationships and the nonlocal inductance

Let us now discuss the numerical results from equations (20) and (21), without the large gap approximation. The current-phase relationships $I_a(\varphi_a, \varphi_b)$, $I_b(\varphi_a, \varphi_b)$ and the inverse inductance matrix Λ_{ij} can be exactly obtained, both at zero and at finite temperature. Compared to uncoupled junctions (SS_a), (SS_b), the cuts of the $I(\varphi_a, \varphi_b)$ along the directions $\varphi_a = \varphi_b$ (resp. $\varphi_a = -\varphi_b$) are dominated by the quartet (resp. pair cotunneling) contributions and their harmonics.

The results depend on the values of the dot couplings $t, \bar{t}$, e.g. of the phase β_R, when there is no direct coupling t_{dd}. For instance, fixing $\beta_R = \frac{\pi}{7}$, both CAR and EC processes contribute. On the other hand, fixing $\beta_R = \frac{\pi}{2}$, EC dominates, and fixing $\beta_R = \pi$, CAR dominates.

In the nonresonant regime, Figure 4 shows the exact result for the inverse nonlocal inductance, approaching the $-\cos(2\varphi)$ regime for large dot energies. Comparing to the perturbative expression equation (28), it is clear from this figure that $E_{PC} > 0$ but $E_Q < 0$, generalizing the analytical large gap result of Section 3.

The resonant regime displays a strong anharmonicity. Figure 5 shows $I_a(\varphi_a = \varphi, \varphi_b = \varphi)$, $I_a(\varphi_a = \varphi, \varphi_b = -\varphi)$ and $\Lambda_{ab}(\varphi_a = \varphi, \varphi_b = \varphi)$, $\Lambda_{ab}(\varphi_a = \varphi, \varphi_b = -\varphi)$. The effect of the interdot coupling is apparent in the $I_a(\varphi_b)$ plots for $\varphi_b = \pm\varphi_a$. One takes as a reference the current $I_{a0}(\varphi_b) = \pm I_{a0}(\varphi_a)$ in absence of interdot coupling and nonlocal effects. For $\varphi_a = \varphi_b$ the nonlocal processes opening a gap at phase π (Fig. 2) smoothen the current jump, and are dominated by a quartet π-component. For $\varphi_a = -\varphi_b$ the splitting of the crossing points give rise to a double jump, showing the nonperturbative nature of CAR and EC couplings.

Similarly, the inductance features shown in Figure 5 can be understood qualitatively from the "large gap" ABS spectra calculated in Section 3 (Fig. 2). The negative peak in $\Lambda_{ab}(\varphi_b)$ along the line $\varphi_a = \varphi_b$ comes from the splitting of the individual ABS by the interdot coupling (Fig. 2, left panels). It has a modified Lorentzian shape, and at zero temperature and for $\tilde{t} \ll \Gamma$ its width scales as $\tilde{t}/\Gamma$ and its height scales as $\Gamma^2/\tilde{t}$. On the other hand, along the line $\varphi_a = -\varphi_b$, the two positive and very sharp symmetric peaks originate from the splitting of the ABS crossing along the phase axis (Fig. 2, right panels). The splitting scales as $\tilde{t}/\Gamma$. The divergence of the nonlocal inductance when the interdot coupling goes to zero is an effect of a degeneracy lifting. It disappears at nonzero temperature, which smoothens all the above structures when $\beta\tilde{t} < 1$. Once more, notice that the results for $E_a = E_b$ and $E_a = -E_b$ are not very different. In particular, taking $E_a = E_b$ does not filter out the CAR processes, just as taking $E_a = -E_b$ does not filter out the EC processes.

4.2 Effect of the circuit inductance

In a circuit where the bijunction is closed by two adjacent loops (Fig. 6), the geometrical inductance matrix

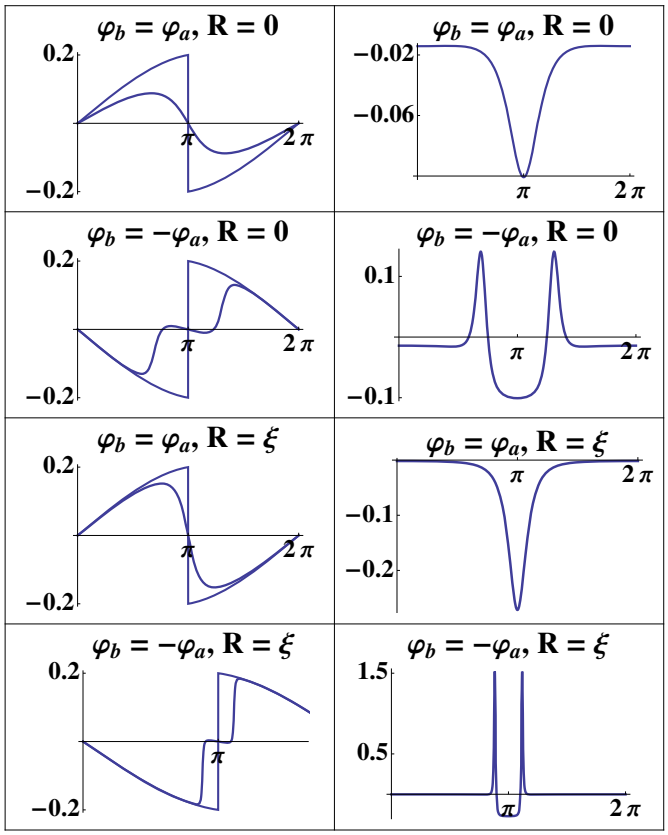

Fig. 5. Current I_a as a function of φ_b (left panels) and nonlocal inverse inductance $\Lambda_{ab} = \frac{\partial I_{Ja}}{\partial \varphi_b}$ (right panels) in the resonant dot case, for $\varphi_b = \pm\varphi_a$, for strong ($R = 0$) and intermediate ($R = \xi$) interdot coupling through S_0. The local resonant current (with a sharp drop at π) is plotted as a reference. Temperature is zero, $E_a = E_b = 0$ and the geometrical phase is $\beta_R = \frac{\pi}{7}$. Notice the sharpening of the structures in Λ_{ab} as the interdot coupling weakens.

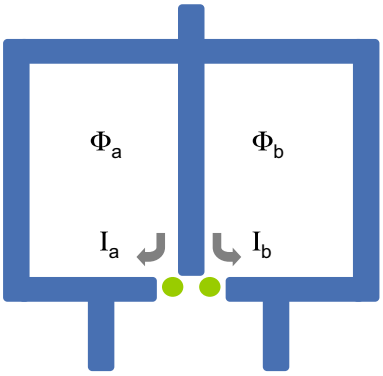

Fig. 6. Scheme of a double dot bijunction inserted into a two-loop and tri-terminal circuit.

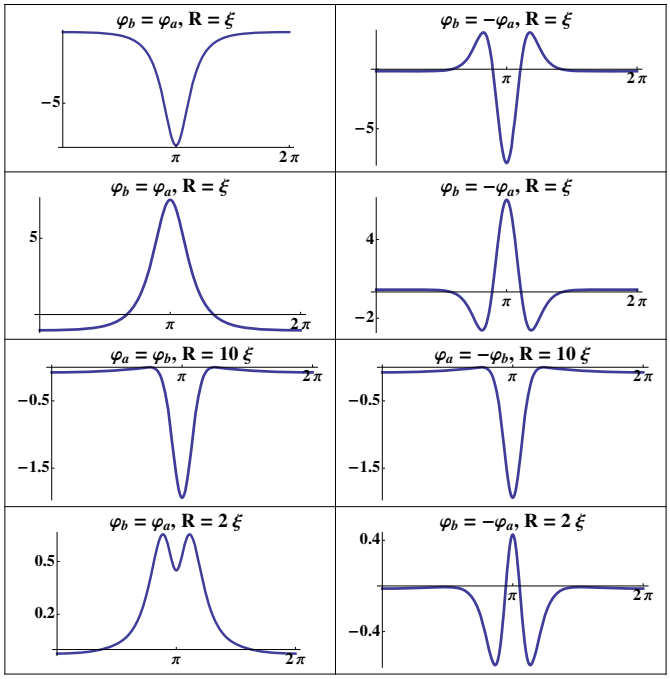

Fig. 7. Effect of self and mutual inductances on the nonlocal inverse inductance (scale $\times 10^2$) for $E_a = E_b = 0, T = 0.02\Delta$. Top line panels: reference curves with nonlocal couplings and no inductance, plotting $\Lambda_{ab}(\varphi_b)$; second line panels: with nonlocal couplings and self, $L_{0aa} = L_{0bb} = 0.2$, plotting $\Lambda_{eab}(\Phi_b)$; third line panels: with self $L_{0aa} = L_{0bb} = 0.2$ and mutual $M_0 = -0.1$, without nonlocal couplings, plotting $\Lambda_{eab}(\Phi_b)$; fourth line panels: with self $L_{0aa} = L_{0bb} = 0.2$ and mutual $M_0 = -0.06$, with nonlocal couplings, plotting $\Lambda_{eab}(\Phi_b)$.

of the circuit should be taken into account, $\mathbf{L}_0 = L_{0aa}, L_{0bb}, L_{0ab} = L_{0ba} = M_0$. In particular, the mutual inductance M_0 couples the pair currents in junctions a and b, and it could interfere with the detection of the quartet and pair cotunneling processes.

Let us consider the double loop circuit pictured in Figure 6. The convention of currents flowing from the central superconductor to the side ones amounts to change the sign of φ_b and I_b, therefore the phase differences φ_a and φ_b are related to the external fluxes Φ_{ea} and Φ_{eb} in loops (a, b) by ($\Phi_0 = \frac{hc}{2e}$):

$$\varphi_a = \frac{2\pi}{\Phi_0}(\Phi_{ea} + L_{0aa}I_a - M_0 I_b),$$

$$\varphi_b = -\frac{2\pi}{\Phi_0}(\Phi_{eb} - L_{0bb}I_b + M_0 I_a). \qquad (32)$$

We define the full inverse nonlocal inductance as $\Lambda_{eij} = \frac{2e}{\hbar}\frac{\partial I_i}{\partial \Phi_{ej}}$, $(i, j = a, b)$. Figure 7 compares this quantity to the one due only to nonlocal couplings, and shows it for several cases. With the self L_{0aa}, L_{0bb} and with nonlocal coupling, the patterns $\Lambda_{eab}(\Phi_b)$ are qualitatively similar to the patterns $\Lambda_{ab}(\varphi_b)$, but inverted owing to the phase and flux sign convention. With the mutual inductance M_0 in addition, but without nonlocal coupling, the pattern is inverted compared to the previous one. This is due to the fact that the mutual inductance is *negative*, e.g. it tends to make the currents flowing in loops a, b cancel in the common branch, while the quartet process favours the *same*

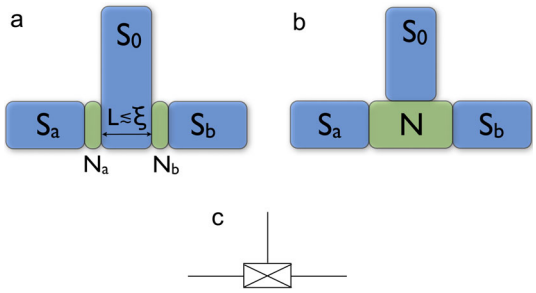

Fig. 8. (a) Scheme of a bijunction made of three superconductors coupling S_0 to S_a and to S_b through normal regions N_a, N_b. Coupling between S_a and S_b is mediated by nonlocal processes through S_0. (b) Bijunction with S_0, S_a, S_b all mutually coupled through a normal region N. (c) Pictorial circuit element scheme for a bijunction.

sign for the currents. Finally, with both nonlocal coupling and mutual inductance, the former is distincly visible, with a dip in the left panel. The marked difference between the two lowest panels of Figure 7 shows that for a realistic circuit the nonlocal processes can be distinguished from the geometric inductances. An alternative to filter out the purely geometric effects is to modulate one or the other of the couplings and operate a synchronous detection.

5 Conclusion

We have calculated the (two current)-(two phase) characteristics of a double dot bijunction, unveiling the anharmonicities occurring in the resonant and degenerate dot level case. The approximate and exact calculations presented in this work enlighten the nature of the proximity effect induced by three superconductors on a double dot forming a Josephson bijunction. We have emphasized the role of the interdot coupling even when the central superconductor is too wide to mediate nonlocal effects. Even a weak coupling between the two junctions, mediated by the central superconductor or by direct interdot tunneling, has strong effects, inducing a measurable nonlocal inductance of purely microscopic origin. In case of a two-loop circuit, it has the opposite sign compared to a geometrical mutual inductance. Alternatively, the current-phase structure can be directly investigated through recently introduced spectroscopy techniques. The Andreev bound state structure is also a necessary basis for understanding the more complicated nonequilibrium behaviour, as investigated in reference [13]. One has to keep in mind nevertheless that the usual adiabatic approximation fails unless the voltages are small enough, and at any voltage in the resonant regime. The phenomenology revealed in a double dot bijunction can be generalized to bijunctions formed with normal metal regions, that can be disconnected (Fig. 8a) or connected (Fig. 8b).

We acknowledge the support of the French National Research Agency, through the project ANR-NanoQuartets (ANR-12-BS1000701). This work has been carried out in the framework of the Labex Archimède (ANR-11-LABX-0033) and of the A*MIDEX project (ANR-11-IDEX-0001-02), funded by the "Investissements d'Avenir" French Government program managed by the French National Research Agency (ANR). We are grateful to T. Kontos for useful discussions.

References

1. M. Tinkham, *Introduction to Superconductivity* (Mc Graw-Hill, Singapore, 1996)
2. M.L. Della Rocca, M. Chauvin, B. Huard, H. Pothier, D. Estève, C. Urbina, Phys. Rev. Lett. **99**, 127005 (2007)
3. L. Bretheau, Ç.Ö. Girit, H. Pothier, D. Estève, C. Urbina, Nature **499**, 312 (2013)
4. B. Dassonneville, M. Ferrier, S. Guéron, H. Bouchiat, Phys. Rev. Lett. **110**, 217001 (2013)
5. A. Cottet, C. Mora, T. Kontos, Phys. Rev. B **83**, 121311 (2011)
6. J.C. Cuevas, H. Pothier, Phys. Rev. B **75**, 174513 (2007)
7. M. Houzet, P. Samuelsson, Phys. Rev. B **82**, 060517 (2010)
8. N.M. Chtchelkatchev, T.I. Baturina, A. Glatz, V.M. Vinokur, Phys. Rev. B **82**, 024526 (2010)
9. A. Freyn, B. Douçot, D. Feinberg, R. Mélin, Phys. Rev. Lett. **106**, 257005 (2011)
10. M. Alidoust, G. Sewell, J. Linder, Phys. Rev. B **85**, 144520 (2012).
11. A.V. Galaktionov, A.D. Zaikin, L.S. Kuzmin, Phys. Rev. B **85**, 224523 (2012)
12. A.V. Galaktionov, A.D. Zaikin, Phys. Rev. B **88**, 104513 (2013)
13. T. Jonckheere, J. Rech, T. Martin, B. Douçot, D. Feinberg, R. Mélin, Phys. Rev. B **87**, 214501 (2013)
14. A. Pfeffer, J.E. Duvauchelle, H. Courtois, R. Mélin, D. Feinberg, F. Lefloch, Phys. Rev. B **90**, 075401 (2014)
15. J. Rech, T. Jonckheere, T. Martin, B. Douçot, R. Mélin, D. Feinberg, Phys. Rev. B **90**, 075419 (2014)
16. D. Gosselin, G. Hornecker, R. Mélin, D. Feinberg, Phys. Rev. B **89**, 075415 (2014)
17. J.-P. Cleuziou, W. Wernsdorfer, V. Bouchiat, T. Ondarcuhu, M. Monthioux, Nat. Nanotechnol. **1**, 53 (2006)
18. L. Hofstetter, S. Csonka, J. Nygård, C. Schönenberger, Nature **461**, 960 (2009)
19. L. Hofstetter, S. Csonka, A. Baumgartner, G. Fülöp, S. d' Hollosy, J. Nygård, C. Schönenberger, Phys. Rev. Lett. **107**, 136801 (2011)
20. L.G. Herrmann, F. Portier, P. Roche, A.L. Yeyati, T. Kontos, C. Strunk, Phys. Rev. Lett. **104**, 026801 (2010)
21. A. Das, Y. Ronen, M. Heiblum, D. Mahalu, A.V. Kretinin, H. Shtrikman, Nat. Commun. **3**, 1165 (2012)
22. J.M. Byers, M.E. Flatté, Phys. Rev. Lett. **74**, 306 (1995)
23. T. Martin, Phys. Lett. **A 220**, 137 (1996)
24. M.P. Anantram, S. Datta, Phys. Rev. B **53**, 16390 (1996)
25. G. Deutscher, D. Feinberg, Appl. Phys. Lett. **76**, 487 (2000)
26. G.B. Lesovik, T. Martin, G. Blatter, Eur. Phys. J. B **24**, 287 (2001)
27. P. Recher, E.V. Sukhorukov, D. Loss, Phys. Rev. B **63**, 165314 (2001)

28. V. Bouchiat, N.M. Chtchelkatchev, D. Feinberg, G.B. Lesovik, T. Martin, J. Torrès, Nanotechnology **14**, 77 (2003)
29. P. Samuelsson, E.V. Sukhorukov, M. Büttiker, Phys. Rev. Lett. **91**, 157002 (2003)
30. R. Mélin, D. Feinberg, Phys. Rev. B **70**, 174509 (2004)
31. D. Beckmann, H.B. Weber, H.V. Löhneysen, Phys. Rev. Lett. **93**, 197003 (2004)
32. S. Russo, M. Kroug, T.M. Klapwijk, A.F. Morpurgo, Phys. Rev. Lett. **95**, 027002 (2005)
33. P.C. Zimansky, V. Chandrasekhar, Phys. Rev. Lett. **97**, 237003 (2006)
34. P. Burset, W.J. Herrera, A. Levy Yeyati, Phys. Rev. B **84**, 115448 (2011)
35. B. van Heck, S. Mi, A.R. Akhmerov, Phys. Rev. B **90**, 155450 (2014)
36. L. Jiang, D. Pekker, J. Alicea, G. Refael, Y. Oreg, F. von Oppen, Phys. Rev. Lett. **107**, 236401 (2011)
37. C. Benjamin, T. Jonckheere, A. Zazunov, T. Martin, Eur. Phys. J. B **57**, 279 (2007)